J. Phys. B: At. Mol. Opt. Phys. **33** (2000) 433–442. Printed in the UK PII: S0953-4075(00)06817-6

On the mechanism of strong-field double photoionization in the helium atom

M Lein†‡, E K U Gross‡ and V Engel†

† Institute of Physical Chemistry, University of Würzburg, Am Hubland, D-97074 Würzburg, Germany

‡ Institute of Theoretical Physics, University of Würzburg, Am Hubland, D-97074 Würzburg, Germany

Received 10 August 1999, in final form 16 November 1999

Abstract. We perform time-dependent quantum calculations on the ionization dynamics of helium in intense ultrashort laser fields. A linear model of the atom is used to extract single- and double-ionization yields for a 780 nm excitation. For an intensity of 10^{15} W cm^{-2} clear evidence is found for a direct double-ionization process which is caused by rescattering of an electron from the core in the presence of the field. A momentum-space analysis of the wavefunctions shows that in this case both electrons are preferentially emitted in the same direction and with different momenta.

1. Introduction

Intense laser pulses with temporal widths in the subpicosecond range have been used to examine the behaviour of atoms and molecules in strong fields thereby revealing a wealth of new and exciting phenomena [1–4]. Of particular interest to atomic physics is the helium atom because it is the simplest atom with electron–electron correlation. In the last decade, intensive theoretical work on the helium atom has yielded highly accurate one-photon single-ionization cross sections [5, 6] and has given new insight into the dynamics of doubly excited states [7–10]. Direct weak-field double photoionization of helium has been investigated experimentally [11] and accurate calculations which fully account for correlation effects have been reported [12, 13]. Also, single- and double-ionization yields resulting from excitation with short and intense laser pulses have been measured by several groups [14–17]. Here, one of the most interesting results is the unexpectedly large rate of double ionization at intensities below the single-ionization saturation. An accurate theoretical description of these processes is very demanding. Ideally one has to solve the time-dependent Schrödinger equation for all particles interacting with an external field. For small laser wavelengths this has been achieved either by expanding the time-dependent wavefunction in an appropriate basis [18, 19] or by using a grid discretization [20, 21]. These calculations use wavelengths up to 380 nm [18], 152 nm [19] and 249 nm [20, 21], respectively. For longer wavelengths, convergence is hard to achieve due to the large-amplitude electronic motion. Therefore, we are currently lacking exact numerical results for the laser parameters of the above-mentioned strong-field experiments.

Several approximations and models have been introduced to tackle the problem and a basic understanding of many aspects concerning the ionization processes has been gained [22–29]. In particular, it has become clear that electron–electron correlation beyond the mean-field picture has to be taken into account to properly describe double ionization.

0953-4075/00/030433+10$30.00

In this paper we use a linear model of helium interacting with an external electric field. This simplification is justified by the fact that the movement of the electrons in a linearly polarized strong field mainly follows the direction of the field. The time-dependent Schrödinger equation is integrated numerically and yields for single and double ionization are calculated. We are primarily interested in the mechanism of double ionization. Two models have been proposed in order to explain the anomalously high double-ionization rates. One possibility [14], usually referred to as *shake-off*, is a fast ionization of a single electron which yields a He^+ ion with the still bound electron in a highly excited state. Since the ionization probability is increased for such an excited electron, the second ionization step takes place immediately. In another model, the double-ionization process occurs when the motion of an outgoing electron is reversed by the field and *rescattering* from the nucleus–electron system takes place [22]. Below we will address the question of how far these models apply.

2. Linear model

Inevitably, not all properties of the helium atom are correctly reproduced by a one-dimensional model. Depending on what kind of physical situation we want to describe, different Hamiltonians are appropriate. For example, in order to obtain doubly excited states corresponding to the *frozen planet configuration* [7] it is essential to retain the singularities of the Coulomb interaction [8, 10]. In the frozen planet configuration, both electrons are localized on the same side of the nucleus. The pure Coulomb interaction between the nucleus and the inner electron is needed to prevent the inner electron from changing to the other side of the nucleus. In a strong laser field of linear polarization, the situation is different because the electrons are able to pass by the nucleus while they oscillate back and forth. Configurations such as the frozen planet orbit are destroyed in a strong field [9]. We estimate the average *transverse* distance of the electrons from the nucleus to be similar to the extension of the ground-state wavefunction which is of the order of 1 au. When going from the real helium atom to a linear model, the bare Coulomb potential

$$v(\boldsymbol{r}) = \frac{1}{|\boldsymbol{r}|} = \frac{1}{\sqrt{z^2+\rho^2}} \tag{1}$$

should be averaged over the transverse coordinate ρ to give a smoothed potential (soft Coulomb interaction) of the form [30]

$$v(z) = \frac{1}{\sqrt{z^2+\epsilon}} \tag{2}$$

with the parameter ϵ set to 1 au according to the estimate above. These considerations apply to the electron–nucleus interaction as well as to the electron–electron interaction. Thus, the Hamiltonian for our two-electron system reads

$$H = -\frac{1}{2}\frac{\partial^2}{\partial z_1^2} - \frac{1}{2}\frac{\partial^2}{\partial z_2^2} - \frac{2}{\sqrt{z_1^2+1}} - \frac{2}{\sqrt{z_2^2+1}} + \frac{1}{\sqrt{(z_1-z_2)^2+1}} + E_0\, f(t)\sin(\omega t)(z_1+z_2) \tag{3}$$

where z_1 and z_2 are the electronic coordinates, E_0 is the peak field strength, $f(t)$ is an envelope function and ω is the laser frequency. Corresponding to an intensity of 10^{15} W cm^{-2} and a wavelength of 780 nm we use $E_0 = 0.169$ au and $\omega = 0.0584$ au. Note that the electronic coordinates can assume positive and negative values which allows for the possibility that both electrons are localized on one side or on different sides of the nucleus. Arguments based on

the quantum uncertainty relation have also been given for the use of a smoothed Coulomb potential [31]. The ionization potential of the system depends on the smoothing parameter ϵ. Consequently, ϵ also influences the calculated ionization yield. On the other hand, we find that all qualitative results of this paper are independent of ϵ.

The linear model has been used before [24, 26, 27, 29] and it was shown that the experimentally obtained knee structure in the cross section for double ionization measured as a function of field intensity is qualitatively reproduced within the approximate treatment [27]. Both in experiment and in the linear model, the 'knee' is roughly located at an intensity of 10^{15} W cm^{-2}, which is the intensity on which we concentrate in this paper. Bauer used the model to calculate spatial electron-probability distributions and concluded that 'Coulomb-repulsion-assisted laser acceleration' is responsible for double ionization, however, at a short wavelength of 114 nm [26].

We integrate the time-dependent Schrödinger equation using the split-operator method [32]. The initial wavefunction is the symmetric ground state, which is obtained by imaginary-time propagation on the given two-dimensional grid. For the results shown in this paper, we used 2100 time steps per laser cycle and grid sizes of about 500×500 au^2. At the edge of the grid, an optical potential absorbs the outgoing electron flux. To obtain ionization yields, we calculate the two-electron current density near the edge (before the electrons enter the absorbing region). Integration of the current density along the boundary gives the probability flux that leaves the grid. At this point, we distinguish between single and double ionization: one of the electrons can be considered as ionized when the boundary at $|z| \sim 250$ au is reached; if the second electron is now located within $|z| < 6$ au we assume single ionization, otherwise double ionization. Then, these single- and double-ionization fluxes are integrated over time. In previous work, ionization probabilities have usually been calculated by integrating over certain regions of the spatial grid. However, our procedure has the advantage that it counts all outgoing electron flux and is therefore unaffected by decay of the norm. In principle, an electron can remain in a bound state even at a large distance from the nucleus. Note, however, that the size of the grid is several times larger than the classical oscillation amplitude $\alpha = E_0/\omega^2 = 50$ au. Thus, if an electron reaches the boundary within the short time scale of $\Delta t \sim 700$ au considered in the calculations below then it must have a drift velocity of at least $v_D \sim \frac{250}{700}$ au ≈ 0.36 au. Such a large momentum cannot be found in a bound state at $z \sim 250$ au. As for double ionization, the results below will explicitly show that both electrons move away from the nucleus with such large momenta that they cannot return or remain bound. This justifies the criterion of 6 au for the second electron.

3. Results

We present calculations for constant laser intensity and for a $\sin^2$-shaped envelope function with a duration of six optical cycles, which corresponds to 15.6 fs. The time dependence of the ionization yields is displayed in figure 1. Note that the time when the curves start to differ from zero depends on the choice of the spatial grid size because the electrons need a finite time to reach the grid boundary where ionization is detected. The functions exhibit a stepwise increase which occurs every half optical cycle. These steps indicate that the electrons leave the grid in the form of wavepackets which are rather narrow in space.

In the case of constant intensity, the very first half-cycle does not produce any noticeable double ionization; the onset of double ionization is delayed relative to single ionization by one half-cycle. The survival probability for neutral He drops to about 10% within five cycles. This implies that the non-sequential double-ionization process $\mathrm{He} \rightarrow \mathrm{He}^{2+} + 2\mathrm{e}^-$ is essentially over by that time, which leads to saturation of the double-ionization curve.

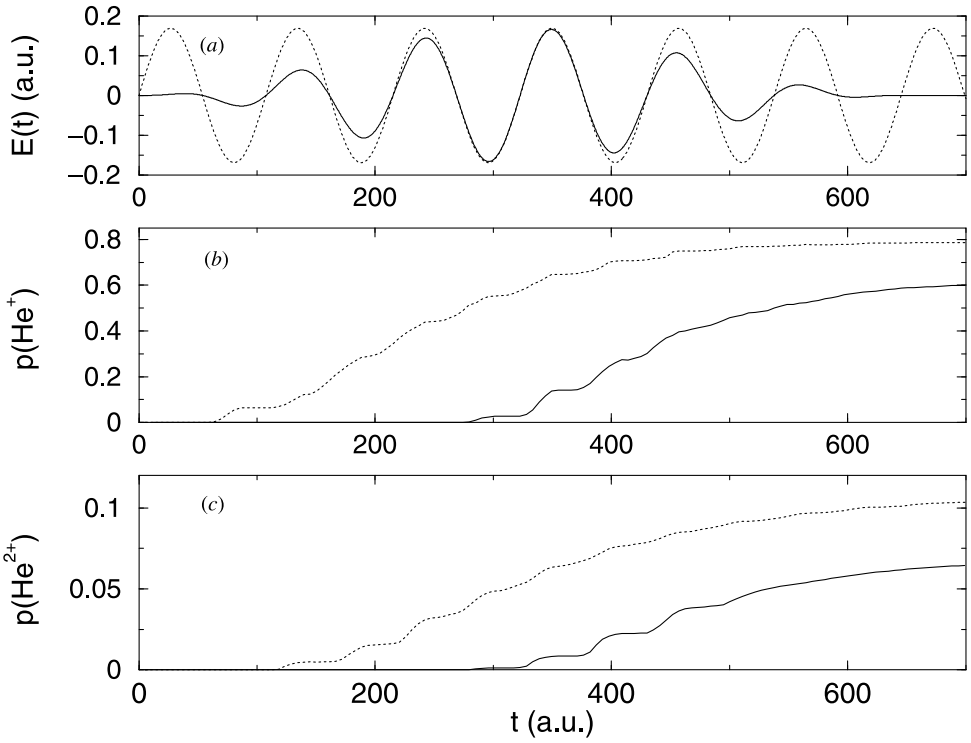

Figure 1. (*a*) Temporal variation of a laser field with constant intensity (broken curve) and of a $\sin^2$-shaped pulse (full curve). The two lower panels show the corresponding time-dependent yields for (*b*) single ionization and (*c*) double ionization.

The $\sin^2$ pulse does not yield noticeable ionization during the first two cycles, since the field is too weak at these early times. Around mid-pulse, single and double ionization become similarly strong as for constant intensity. After the end of the pulse, the ionization yield continues to increase slightly due to the presence of slowly moving ionized electrons which are now reaching the grid boundary.

Next we consider the time-dependent momentum-space wavefunction. We first discuss the case of constant intensity. Figure 2 displays the modulus squared of the wavefunction depending on the electron momenta p_1, p_2 at selected times during the first four periods T of the laser field. At time $T/2$ there is no observable density in the areas where both momenta have large (positive or negative) values which expresses the fact that at this time the probability for double ionization is very small (see figure 1). Note that even though in figure 1 the single-ionization yield is also small at $T/2$, there is a considerable increase at $t \sim 75$ au when the electron flux corresponding to single ionization reaches the grid boundary. In the double-ionization curve, this first steplike increase is completely missing. However, when the first optical cycle is finished the momentum distribution exhibits two small satellites centred at momentum values of about $(p_1, p_2) = (5, 3)$ au. After another half-cycle (at time $1.5T$) similar structures are visible, but now at negative values of the momenta. After two complete cycles the wavefunction becomes much more structured but nevertheless contains clear features around larger positive momenta than at time T. For later times, the system evolves in a very similar fashion except that no more probability density is found in the region where the ground state (figure 2(*a*)) resides. We find that the momentum values where the double-ionization

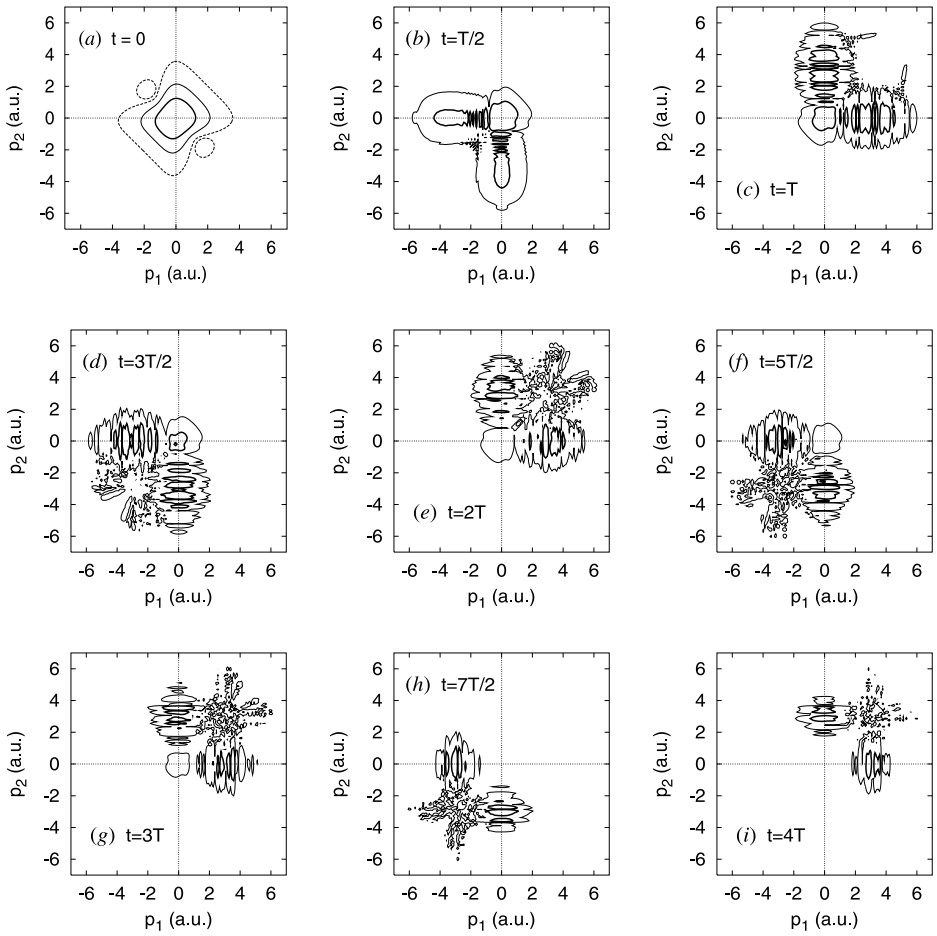

Figure 2. Modulus squared of the momentum-space wavefunctions at selected times t during the action of a constant-intensity laser field with optical period T. Contour-line levels: thick curve, 4×10^{-2}; thin curve, 2×10^{-3}; broken curve, 2×10^{-5}.

structures are located are very weakly dependent on the smoothing parameter ϵ.

The conclusion from the behaviour found in figure 2 is that double ionization is effective every half period, which is consistent with what can be inferred from figure 1. At these times both electrons are emitted with different momenta in the same spatial direction. The process of two electrons emerging with momenta pointing in different directions is negligible. We note in passing that this behaviour changes if different intensities or wavelengths are employed in the calculation. Indeed, previous studies have shown examples of double ionization where electrons are ejected towards opposite sides [24, 26]. In [26] a much shorter wavelength of 114 nm was employed which explains the different behaviour observed in that study. On the other hand, the wavelength used in [24] was 911 nm, which is not too different from our 780 nm. With an intensity of 3.15×10^{15} W cm^{-2}, however, those calculations are clearly beyond the single-ionization saturation as can be seen from the intensity-dependent calculations in [27]. Consequently, *sequential* double ionization is the dominant process there, in contrast to the *non-sequential* process found in the present study. For the short wavelength of

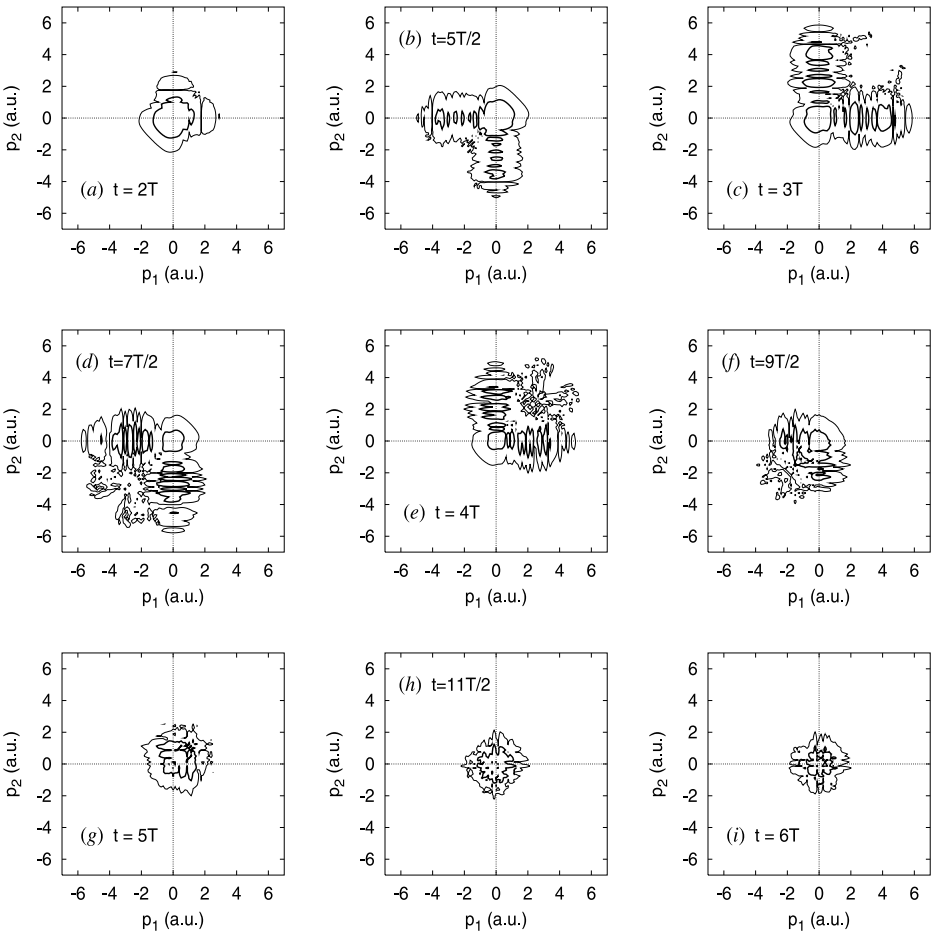

Figure 3. Modulus squared of the momentum-space wavefunctions at selected times t during the action of a $\sin^2$-shaped pulse with optical period T. Contour-line levels: thick curve, 4×10^{-2}; thin curve, 2×10^{-3}.

193 nm, it has already been observed that sequential ionization preferentially leads to ejection in opposite directions, whereas the non-sequential process favours ejection on the same side [20].

If both electrons are emitted at the same time and in the same direction, as is the case here, then we can understand that, as a consequence of the Coulomb repulsion, the electrons try to avoid each other by leaving with different velocities.

In figure 3, the momentum distribution during the interaction with the $\sin^2$ pulse is shown for selected times starting at $t = 2T$. Between $t = 5T/2$ and $t = 4T$ (panels (b)–(e)), i.e. when the laser amplitude is close to the peak amplitude, the momentum distributions are amazingly similar to those in figures $2(b)$–(e). Afterwards, on the falling edge of the pulse, no more structures appear at large momenta, indicating that ionization comes to an end. Comparing figures 2 and 3, we conclude that pulse-shape effects on the ionization mechanism are small. As soon as the intensity is large enough to cause single or double ionization, these processes take place without being influenced much by the previous evolution. We have found the same

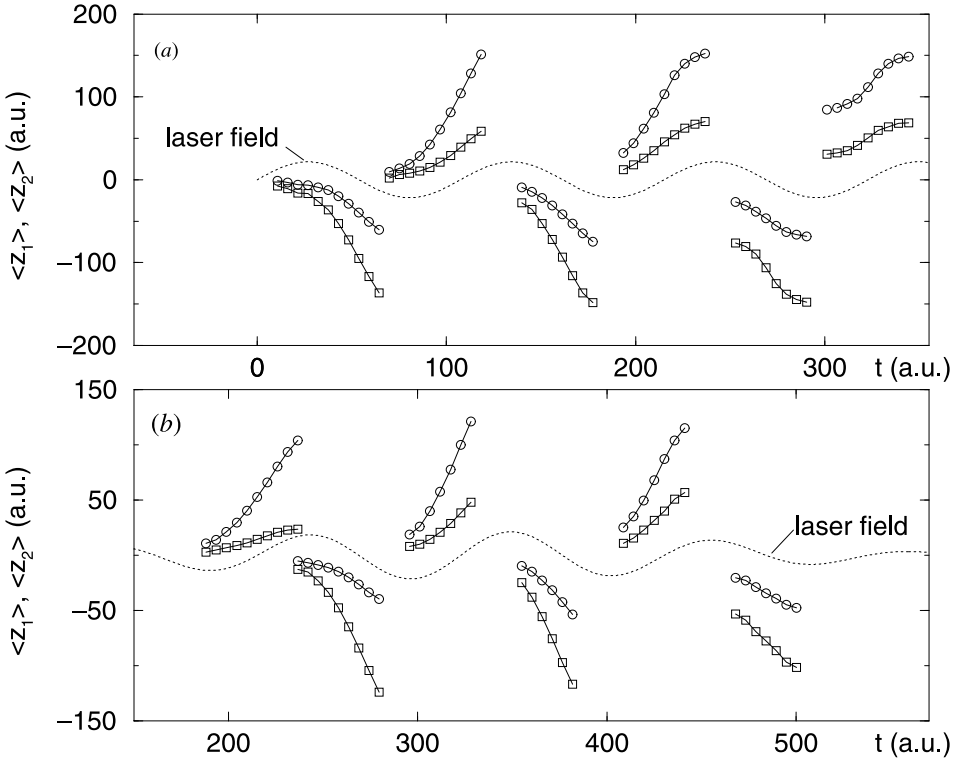

Figure 4. Electron-coordinate expectation values $\langle z_1 \rangle$ (–○–) and $\langle z_2 \rangle$ (–□–) calculated for parts of the spatial wavefunction describing double ionization (see text): (*a*) field with constant intensity, (*b*) $\sin^2$-shaped pulse. For orientation, the laser field is plotted in arbitrary units.

trends for even shorter pulse durations.

Figure 4 shows position expectation values $\langle z_1 \rangle$, $\langle z_2 \rangle$ calculated in the triangles where $\{z_1, z_2 > 6$ au; $z_2 < z_1\}$ and $\{z_1, z_2 < -6$ au; $z_2 < z_1\}$. The electron probability located in these regions corresponds to a double-ionization process with both electrons on the same side of the nucleus. By choosing $z_2 < z_1$ we select one of the electrons as the outer one. Otherwise the symmetry of the wavefunction would always lead to $\langle z_1 \rangle = \langle z_2 \rangle$. Figures 4(*a*) and (*b*) show the constant-intensity case and the $\sin^2$ case, respectively. The two time axes have been arranged such that those times that we expect to exhibit similar ionization dynamics (see figures 2 and 3) are placed at the same horizontal position, i.e. $t = 0$ of (*a*) is directly above $t = 2T$ of (*b*). A comparison of both panels confirms the similarity.

Obviously, in double ionization, both expectation values $\langle z_1 \rangle$, $\langle z_2 \rangle$ become large simultaneously. However, the figure clearly shows that they increase with a different rate, i.e. the electrons have different velocities. This is consistent with what was found from the momentum-space analysis above. The precise value of the electron velocities should not be extracted from figure 4 because some electron flux may always move into or out of the triangular regions. Although in figure 4(*a*) the time dependence of $\langle z_1 \rangle$ and $\langle z_2 \rangle$ is similar for all shown half-cycles, the double-ionization yield produced by the first half-cycle is two orders of magnitude lower than that produced at later times and therefore not visible in figure 1. Neither are the processes seen in figure 4(*b*) at times before $t \sim 250$ au.

The temporal behaviour of the expectation values seems to indicate that double ionization

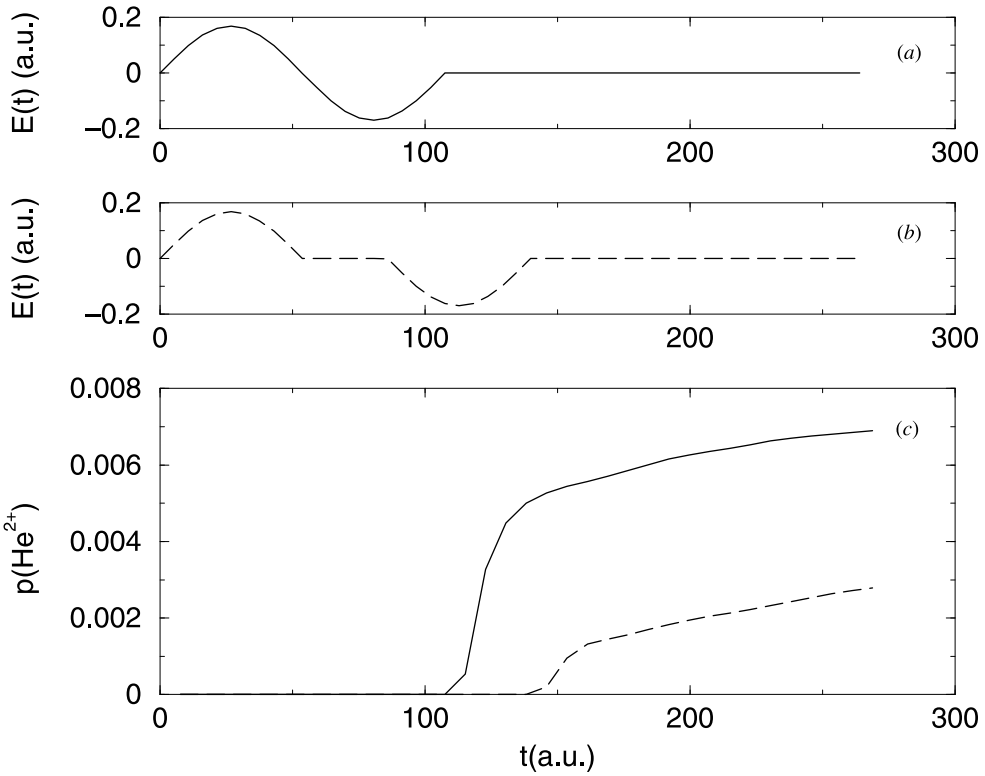

Figure 5. The upper panels show the time dependence of (*a*) a one-cycle 'pulse' and (*b*) another where the second half-cycle is time-delayed with respect to the first one. The resulting double-ionization yields are plotted in panel (*c*). The line style distinguishes case (*a*) from case (*b*).

originates when both electrons are close together (at least at times before the ground state is depleted), so that the process is initialized by field-assisted scattering of one electron from the core. If this is true, then the rate for double ionization must decrease if the electron which is to be scattered is further away from the core at the time when the laser field interacts with the still bound electron. To show this effect we consider the interaction with two different 'one-cycle pulses' as displayed in figure 5. The first one acts continuously with the atoms (panel (*a*)) whereas in the second case the field is switched off for a while after the first half-cycle (panel (*b*)). Panel (*c*) of the figure shows the double-ionization curves obtained in either case. It is seen that the ionization is suppressed in the case where the second half-cycle is time-delayed versus the first. The interpretation is as follows: the first half-cycle creates an outgoing electron. The second half-cycle reverses the direction of this electron for possible backscattering. In the time-delayed case, however, the electron has time to travel away from the core, reducing the probability for electron–core collision. In contrast, the ionization of an excited core (shake-off) does *not* depend on the distance of the outgoing electron. Therefore, the observed suppression proves that e–2e scattering is the major origin of double ionization. From the figure, its contribution is estimated to be at least 60%.

The remaining double-ionization probability may be due to a shake-off process. It can also be caused by an excitation of the two-electron system in the first half-cycle (without ionization) followed by simultaneous ejection of both electrons during the second half-cycle. Since figure 4 has shown that the electrons leave from the nucleus practically simultaneously,

we consider the shake-off mechanism to be unlikely.

4. Conclusion

We have shown that in the employed linear model rescattering of an electron in an intense short laser field with 780 nm wavelength and an intensity of 10^{15} W cm^{-2} is the main reason for double ionization. In this case we find that both electrons emerge with different momenta from one and the same side of the nucleus. The results were obtained by solving the time-dependent Schrödinger equation including full electron–electron correlation. The linear model uses a soft Coulomb potential which allows a passage of the electrons along the nucleus. We believe that the model is quite realistic and predicts the mechanism for double ionization reliably. However, we have to keep in mind that the transfer of many quanta of angular momentum to the electrons decreases the influence of the rescattering process on the ionization. Consequently, the effect of rescattering should be somewhat stronger in the linear model than in a real helium atom, therefore enhancing double ionization and also the survival of bound two-electron configurations at the cost of single ionization.

Acknowledgment

Financial support from the Deutsche Forschungsgemeinschaft (Schwerpunktprogramm 'Time-dependent phenomena and methods in quantum systems of physics and chemistry', EN 241/6-1) is gratefully acknowledged.

References

[1] Gavrila M (ed) 1992 *Atoms in Intense Laser Fields* (New York: Academic)
[2] Piraux B, L'Huillier A and Rzążewski K (ed) 1993 *Super-Intense Laser–Atom Physics (SILAP) III* (New York: Plenum)
[3] Bandrauk A D (ed) 1994 *Molecules in Laser Fields* (New York: Dekker)
[4] Lambropoulos P, Maragakis P and Zhang J 1998 *Phys. Rep.* **305** 203
[5] Wintgen D and Delande D 1993 *J. Phys. B: At. Mol. Opt. Phys.* **26** L399
[6] Grémaud B and Delande D 1997 *Europhys. Lett.* **40** 363
[7] Richter K, Briggs J S, Wintgen D and Solov'ev E A 1992 *J. Phys. B: At. Mol. Phys.* **25** 3929
[8] López-Castillo A, de Aguiar M A M and Ozorio de Almeida A M 1996 *J. Phys. B: At. Mol. Phys.* **29** 197
[9] Schlagheck P and Buchleitner A 1998 *J. Phys. B: At. Mol. Opt. Phys.* **31** L489
[10] Schlagheck P and Buchleitner A 1999 *Europhys. Lett.* **46** 24
[11] Schwarzkopf O, Krässig B, Elmiger J and Schmidt V 1993 *Phys. Rev. Lett.* **70** 3008
[12] Teng Z and Shakeshaft R 1993 *Phys. Rev.* A **47** R3487
[13] Maulbetsch F and Briggs J S 1993 *J. Phys. B: At. Mol. Opt. Phys.* **26** 1679
[14] Fittinghoff D N, Bolton P R, Chang B and Kulander K C 1992 *Phys. Rev. Lett.* **69** 2642
[15] Walker B, Mevel E, Yang B, Breger P, Chambaret J P, Antonetti A, DiMauro L F and Agostini P 1993 *Phys. Rev.* A **48** R894
[16] Kondo K, Sagisaka A, Tamida T, Nabekawa Y and Watanabe S 1993 *Phys. Rev.* A **48** R2531
[17] Walker B, Sheehy B, DiMauro L F, Agostini P, Schafer K J and Kulander K C 1994 *Phys. Rev. Lett.* **73** 1227
[18] Zhang J and Lambropoulos P 1995 *J. Phys. B: At. Mol. Opt. Phys.* **28** L101
[19] Scrinzi A and Piraux B 1997 *Phys. Rev.* A **56** R13
[20] Taylor K T, Parker J S, Dundas D, Smyth E and Vivirito S 1999 *Laser Phys.* **9** 98
[21] Dundas D, Taylor K T, Parker J S and Smyth E S 1999 *J. Phys. B: At. Mol. Opt. Phys.* **32** L231
[22] Corkum P B 1993 *Phys. Rev. Lett.* **71** 1994
[23] Becker A and Faisal F H M 1996 *J. Phys. B: At. Mol. Opt. Phys.* **29** L197
[24] Lappas D G, Sanpera A, Watson J B, Burnett K, Knight P L, Grobe R and Eberly J H 1996 *J. Phys. B: At. Mol. Opt. Phys.* **29** L619
[25] Watson J B, Sanpera A, Lappas D G, Knight P L and Burnett K 1997 *Phys. Rev. Lett.* **78** 1884

[26] Bauer D 1997 *Phys. Rev.* A **56** 3028
[27] Lappas D G and van Leeuwen R 1998 *J. Phys. B: At. Mol. Opt. Phys.* **31** L249
[28] Becker A and Faisal F H M 1999 *Phys. Rev.* A **59** R1742
[29] Liu W-C, Eberly J H, Haan S L and Grobe R 1999 *Phys. Rev. Lett.* **83** 520
[30] Grobe R and Eberly J H 1993 *Phys. Rev.* A **48** 4664
[31] Rzążewski K, Lewenstein M and Salières P 1994 *Phys. Rev.* A **49** 1196
[32] Feit M D, Fleck J A and Steiger A 1982 *J. Comput. Phys.* **47** 412